Ring Expansion and Isomerization in *N*-Methylindole and *N*-Methyleneindole Radical. Quantum Chemical and Kinetics Calculations

Faina Dubnikova and Assa Lifshitz*

Department of Physical Chemistry, The Hebrew University, Jerusalem 91904, Israel

Received: December 31, 2003

Ring expansion and isomerization in *N*-methylindole and *N*-methyleneindole were studied by the Becke three-parameter hybrid method with Lee−Yang−Parr correlation functional approximation (B3LYP). Structure, energy, and frequency calculations were carried out with the Dunning correlation-consistent polarized double-ζ (cc-pVDZ) basis set. The reaction leading to ring expansion in *N*-methyleneindole proceeds via an intermediate that with an additional transition state produces hydroquinoline radical. The latter, by a fast H-atom ejection forms quinoline. The intermediate consists of a newly formed three-membered ring fused to the five-membered pyrrole ring. Isoquinoline production proceeds via an intermediate containing three rings fused together that increases the energetics of the process in comparison with quinoline production. Several transition states and intermediates are common to both ring expansion and isomerization of *N*-methyleneindole so that there are competing parallel pathways that determine the final distribution among the isomerization and ring expansion products. Potential energy surfaces for interisomerization among the various isomers of methylindole were calculated, and several reaction pathways are suggested. Ring expansion in the molecule of *N*-methylindole does take place, but its energy barrier is very high. The reaction coordinate in this process is cleavage of the C−N bond and one of the C−H bonds of the methyl group that from a kinetics viewpoint is equivalent to ejection of a H-atom from the molecule and ring expansion from *N*-methyleneindole radical. Rate constants for isomerization and ring expansion were obtained by transition-state theory, applying multiwell calculations with computer modeling. The structure, energetics, and additional parameters on the potential energy surfaces and the rate constants for the various processes are reported.

I. Introduction

It has been shown that methyl group shifts and ring expansion to form quinoline are important reaction products of *N*-methylindole[1] when the latter is elevated to high temperature, for example, by shock heating. The second isomer of ring expansion, isoquinoline, was not observed among the products of postshock mixtures.[1]

We have recently published detailed quantum chemical calculations on the ring expansion processes in three five-membered rings: methylpyrrole,[2] methylcyclopentadiene,[3] and methylindene.[4,5] It was shown that the lowest energy pathways for ring expansion are in the isomers where the methylene group is connected to an sp^3 carbon or nitrogen. The other isomers undergo ring expansion via isomerization to N- or sp^3-substituted radicals, rather than via direct reaction.

The purpose of this investigation is to find reaction pathways for two processes, methyl group shifts and ring expansion in *N*-methylindole, and to calculate the energetics and the structure of the transition states and intermediates on the potential energy surfaces. Its purpose is also to evaluate the unimolecular rate constants of the various processes. It will be interesting to find differences and similarities in the ring expansion processes in methylindene and methylindole and also to elucidate the effect of a fused benzene ring to the five-membered ring. It will also be interesting to rationalize the absence of isoquinoline among the reaction products in shock-heated mixtures of *N*-methylindole.

II. Computational Details

1. Quantum Chemical Calculations. We used the Becke three-parameter hybrid method[6] with Lee−Yang−Parr correlation functional approximation with unrestricted open shell wave functions (uB3LYP)[7] and the Dunning correlation-consistent polarized valence double-ζ (cc-pVDZ) basis set.[8] Optimization of the ground-state geometry of the radical species was done using the Berny geometry optimization algorithm.[9] For determining transition-state structures, we used the combined synchronous transit-guided quasi-Newton (STQN) method.[10] Higher level calculations were done using these geometries.

All the calculations were performed without symmetry restrictions. Vibrational analyses were done at the same level of theory to characterize the optimized structures as local minima or transition states. Calculated vibrational frequencies and entropies (at the uB3LYP level) were used to evaluate pre-exponential factors of the reactions under consideration. All the calculated frequencies, the zero-point energies, and the thermal energies are of harmonic oscillators. The calculations of the intrinsic reaction coordinate (IRC), to check whether the transition states under consideration connect the expected reactants and products, were done at the uB3LYP level of theory with the same basis set as was used for the stationary point optimization. It was verified that each transition state has one imaginary frequency.

Each optimized uB3LYP structure was recalculated at a single-point quadratic CI including single and double substitutions with a triple contribution to the energy—uQCISD(T).[11]

10.1021/jp031360m CCC: $27.50
Published on Web 06/19/2004

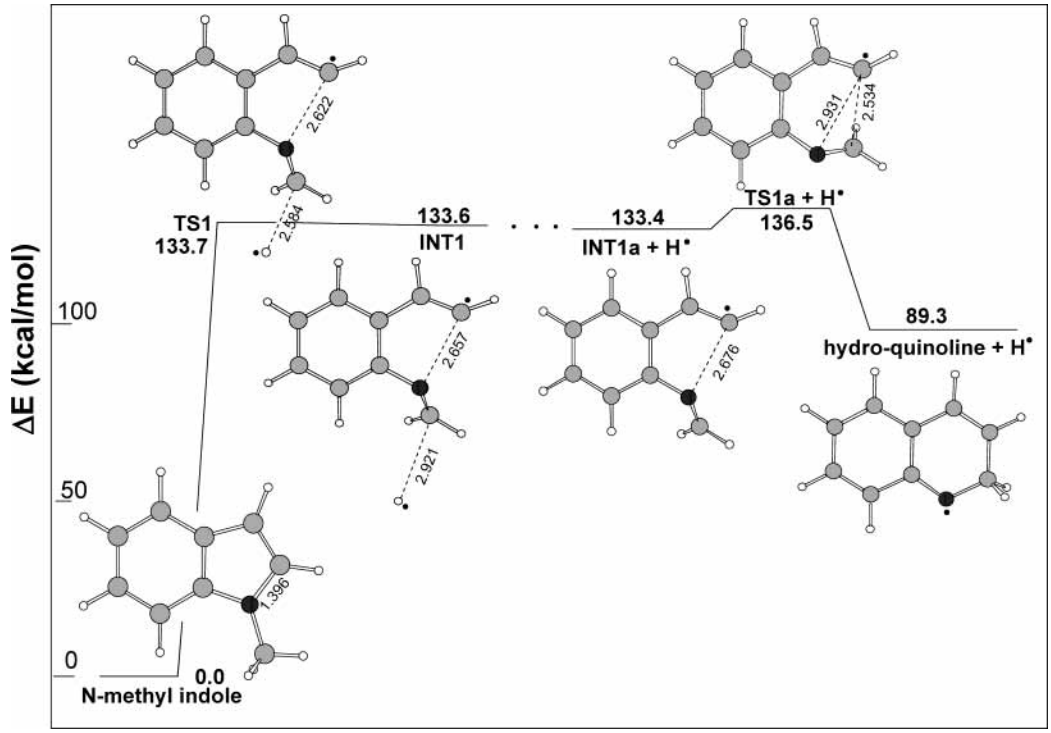

Figure 1. Potential energy surface of *N*-methylindole ring expansion. Relative energies (kcal/mol) are calculated at the uB3LYP/cc-pVDZ level of theory. Bond distances are given in angstroms.

All of the reported relative energies include zero-point energy (ZPE) correction.

The DFT and QCISD(T) computations were carried out using the Gaussian-98 program package[12] and were done on a DEC Alpha XP1000 1/667 professional workstation.

2. Rate Constant Calculations. To evaluate the high-pressure limit first-order rate constants from the results of the quantum chemical calculations the relation

$$k_\infty = \sigma(kT/h)\exp(\Delta S^{\ddagger}/R)\exp(-\Delta H^{\ddagger}/RT)$$

was used,[13,14] where h is the Planck constant, k is the Boltzmann factor, σ is the degeneracy of the reaction coordinate, and $\Delta H^{\ddagger}$ and $\Delta S^{\ddagger}$ are the temperature-dependent enthalpy and entropy of activation, respectively. Since we deal with unimolecular reactions, $\Delta H^{\ddagger} = \Delta E^{\ddagger}$, where $\Delta E^{\ddagger}$ is the energy difference between the transition state and the reactant. $\Delta E^{\ddagger}$ is equal to $\Delta E^0_{\text{total}} + \Delta E_{\text{thermal}}$, where $\Delta E^0_{\text{total}}$ is obtained by taking the difference between the total energies of the transition state and the reactant and $\Delta E_{\text{thermal}}$ is the difference between the thermal energies of these species.

III. Results and Discussion

1. Ring Expansion. *A. Ring Expansion in N-Methylindole.* As has been mentioned before, in our studies on the ring expansion in *N*-methylpyrrole we found that the process can proceed from both the molecule and its radical *N*-methylenepyrrole. The latter is formed by H-atom abstraction or ejection in a high-temperature environment, for example, behind shock waves. The potential energy surface of the ring expansion from the molecule *N*-methylindole is shown in Figure 1. The first stage on this surface, TS1, is rupture of the N−C bond together with practically breaking one of the C−H bonds in the methyl group by increasing its distance to 2.584 Å (Figure 1). This is an open-shell singlet transition state. There is no charge separation, and the electron density on the extended hydrogen atom is 0.007, which is practically zero. The transition state TS1 leads to an intermediate, INT1, with a structure and energetics very similar to those of TS1. Locating a transition state going from INT1 to INT1a requires a variational-transition-state (VTS) calculation. However, this was not done since the C−H bond is so much extended that there will be practically no barrier for the process.

The final stage on the surface is the production of hydroquinoline. The main point in this potential energy surface is the very high energy level (∼134 kcal/mol) of TS1. It simply suggests that ring expansion from methylindole is composed of two processes, namely, C−H bond breaking, which forms a radical intermediate, and C−N bond rupture. We could not find a transition state where the C−N bond is broken without an extension of the C−H bond. We also tried to calculate a transition state on a triplet potential energy surface to find out whether there is a low-lying triplet transition state that can lead to ring expansion with a lower barrier. We did find a triplet transition state, but its energy level was even higher, ∼141 kcal/mol.

Since in the high-temperature environment the radical intermediate can be obtained by other means such as free radical reactions, and their concentrations can be quite high, the ring expansion will take place practically only from the radical intermediates.

B. N-Methyleneindole → Hydroquinoline. The potential energy surface of this process, as shown in Figure 2, contains two transition states (TS2 and TS3) and one intermediate (INT2). Other important parameters of this reaction are listed in Table 1. The first step is the production of an intermediate that is very similar to the equivalent intermediates in the processes of the ring expansion in 5-methylenecyclopentadiene,[3] *N*-methylenepyrrole,[2] and 1-methyleneindene.[5] These intermediates are

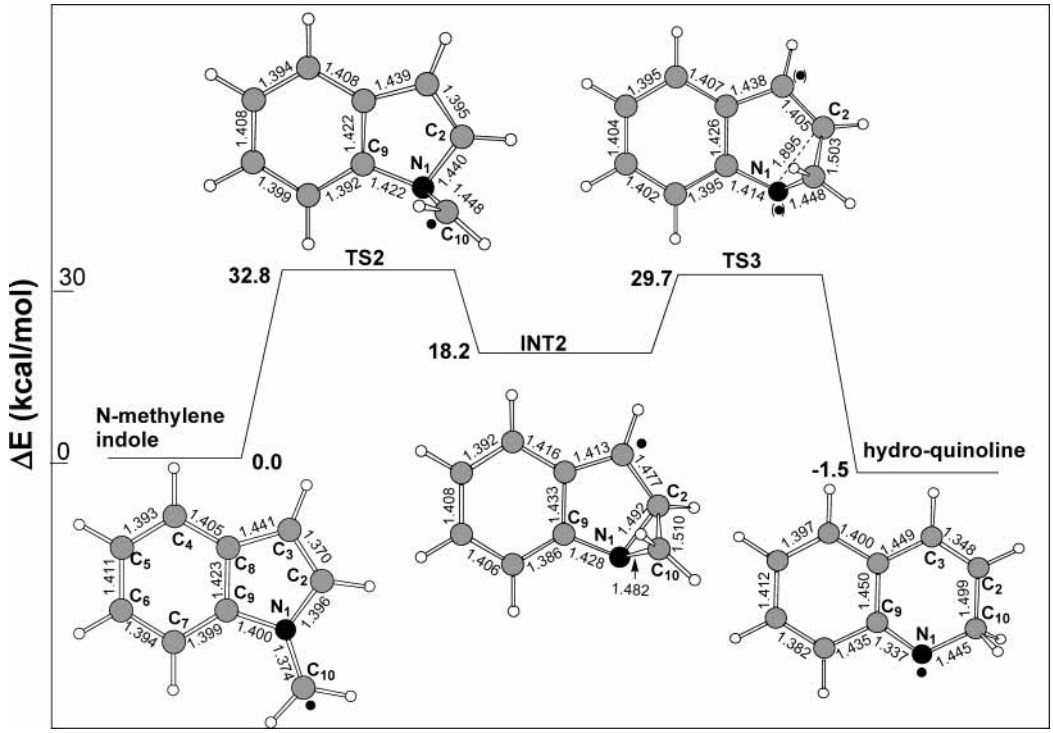

Figure 2. Reaction pathway for *N*-methyleneindole → hydroquinoline ring expansion. Relative energies (kcal/mol) are calculated at the uQCISD(T)// uB3LYP/cc-pVDZ level of theory. Bond distances are given in anstroms. The symbol (●) denotes partially distributed free electron density.

TABLE 1: Total Energies E_{total} (au), Zero-Point Energies, Relative Energies ΔE,[a] Imaginary Frequencies,[b] and Entropies[c] of the Species on the *N*-Methyleneindole → Hydroquinolyl and *N*-Methyleneindole → Hydroisoquinolyl Ring Expansion and *N*-methyleneindole → 2-Methyleneindole Isomerization Surfaces, Calculated at the uB3LYP/cc-pVDZ and uQCISD(T)/ cc-pVDZ//uB3LYP/cc-pVDZ Levels of Theory

	uB3LYP					uQCISD(T)	
species	E_{total}	ΔE^a	ZPE	S^c	ν^b	E_{total}	ΔE^a
			N-Methyleneindole → Hydroquinoline Ring Expansion				
N-methyleneindole	−402.497449	0.0	89.6	88.4		−401.342916	0.0
TS2	−402.443832	32.9	88.8	84.3	(i-639)	−401.285516	32.8
INT2	−402.464841	21.1	90.3	84.0		−401.314470	18.2
TS3	−402.447392	31.4	89.6	83.7	(i-579)	−401.295648	29.7
hydroquinoline	−402.501821	−2.0	90.3	85.7		−401.346551	−1.5
			N-Methyleneindole → Hydroisoquinoline Ring Expansion				
N-methyleneindole	−402.497449	0.0	89.6	88.4		−401.342916	0.0
TS4	−402.430527	41.1	88.7	83.9	(i-593)	−401.278982	39.2
INT3	−402.438467	37.1	89.6	84.3		−401.290521	32.9
TS5	−402.434345	39.3	89.2	83.3	(i-448)	−401.284727	36.2
Hydroisoquinoline	−402.509033	−6.3	90.5	86.7		−401.354680	−6.4
			N-Methyleneindole → 2-Methyleneindole Isomerization				
N-methyleneindole	−402.497449	0.0	89.6	88.4		−401.342916	0.0
TS2	−402.443832	32.9	88.8	84.3	(i-639)	−401.285516	32.8
INT2	−402.464841	21.1	90.3	84.0		−401.314470	18.2
TS6	−402.431250	40.2	88.3	84.8	(i-446)	−401.277618	39.7
INT4	−402.498624	35.6	88.3	90.1		−401.295975	28.2
TS7	−402.416945	47.4	86.4	86.3	(i-1324)	−401.258360	49.9
2-methyleneindole	−402.519795	−14.0	90.0	86.7		−401.360094	−10.3

[a] Relative energies in kcal/mol. $\Delta E = \Delta E_{total} + \Delta(ZPE)$. [b] Imaginary frequency in cm^{-1}. [c] Entropies at 298 K in cal/(K·mol).

characterized by bicyclic structures with five- and three-membered rings fused together.

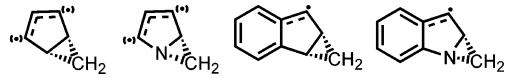

In transition state TS2, which leads to intermediate INT2 (Figure 2), the geometrical parameters and electron density distribution have values between those of *N*-methyleneindole and intermediate INT2. The reaction coordinate in TS2 is a C(10)−N(1)−C(2) angle bend that brings C(10) and C(2) close together and a rotation of the methylene group with respect to the ring plane. The methylene group movement causes a deformation in the pyrrole ring. The energy barrier for production of this fused ring intermediate is 32.8 kcal/mol at the uQCISD(T)//uB3LYP/cc-pVDZ level of theory. This value is very close to the similar barrier on the methylenepyrrole surface, which is 33.3 kcal/mol at the same level of theory.[2] The intermediate INT2 produces hydroquinoline via transition state TS3. The reaction coordinate is a N(1)−C(2) bond cleavage

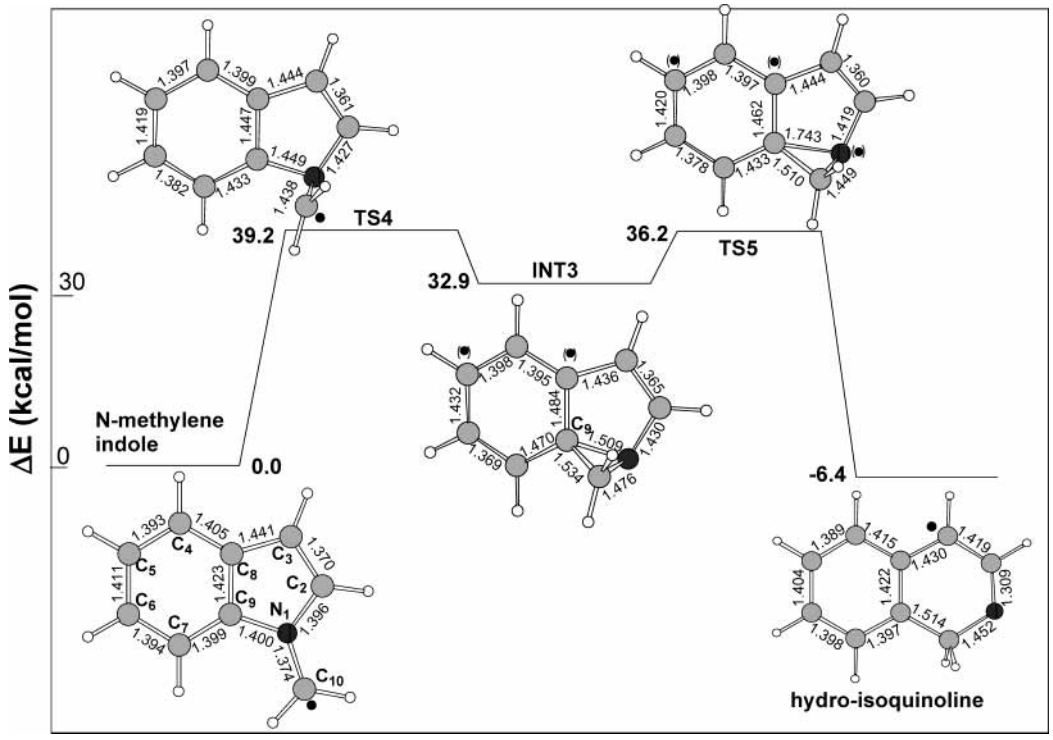

Figure 3. Reaction pathway for *N*-methyleneindole → hydroisoquinoline ring expansion. Relative energies (kcal/mol) are calculated at the uQCISD(T)//uB3LYP/cc-pVDZ level of theory. Bond distances are given in angstroms. The symbol (●) denotes partially distributed free electron density.

together with a N(1)−C(10)−C(2) angle bend. N(1)−C(2) is the bridge across which the three- and five-membered rings are fused together. The energy barrier for INT1 → hydroquinoline is ∼12 kcal/mol. The very low barrier for the N−C bond rupture is the result of the large amount of strain energy that is released from the two fused rings in INT2.

It should be mentioned that both transition states and the intermediate on the potential energy surface here are at considerably higher energy levels than the similar species on the corresponding surfaces of 5-methylenecyclopentadiene and 1-methyleneindene, which do not contain nitrogen as a heteroatom. For example, the first barrier that characterizes the methylene group movement in 5-methylenecyclopentadiene is ∼12 kcal/mol and in methyleneindene ∼9 kcal/mol as compared to ∼33 kcal/mol in methylenepyrrole and methyleneindole. This difference is caused by a considerable loss of aromaticity of the pyrrole ring that expresses itself by a deviation of the N(1)−C(10) bond from the pyrrole ring plane. Another difference between *N*-methyleneindole and TS2 is the length of the three N−C bonds in these two species. N(1)−C(10) increases from 1.374 to 1.448 Å, N(1)−C(2) from 1.398 to 1.440 Å, and N(1)−C(9) from 1.400 to 1.442 Å. The loss of aromaticity also applies to intermediate INT2 and TS3.

The final stage of the process is an H-atom ejection from hydroquinoline radical to produce quinoline. The structure of hydroquinoline radical contains a benzene ring fused to a nonplaner six-membered ring with two double bonds, N(1)−C(9) and C(2)−C(3). The electron density is concentrated solely on N(1). The C(10)−H(8) and C(10)−H(9) bonds are both equal to 1.113 Å as compared to 1.085 Å in *N*-methyleneindole. The increased bond lengths indicate a weakening of these two bonds that facilitates the ejection of one hydrogen atom and the formation of quinoline. It should be mentioned that the ejection of the hydrogen atom from hydroquinoline does not have the variational transition state since the attachment of a hydrogen atom to quinoline has a barrier owing to the decrease in the resonance energy of quinoline.

C. N-methyleneindole → Hydroisoquinoline. As has been shown the insertion of C(10) into the bond N(1)−C(2) yields hydroquinoline (Figure 2). The insertion of C(10) into the N(1)−C(9) bond yields hydroisoquinoline. The potential energy surface of this process is shown in Figure 3, and some other important parameters are listed in Table 1. This surface contains two transition states and one intermediate and is very similar to the one that describes the production of hydroquinoline. However, there is a marked difference in the stability of the intermediates on the two surfaces. Whereas in INT2 on the hydroquinoline potential energy surface (Figure 2) we find only pairs of rings fused together, on the hydroisoquinoline surface, INT3 has three rings fused together, which inserts a considerable strain on the structure and thus increases the energy level of both INT3 and TS4 (Figure 3). Moreover, in both TS4 and INT3 there is some loss of resonance energy of the benzene ring in addition to that in the pyrrole ring. This is caused by the fact that the carbon atom C(9), which is common to both the pyrrole and benzene rings, becomes an sp^3 carbon and thus cannot form a double bond.

The difference between the energy levels of intermediates INT3 and INT2 is approximately 15 kcal/mol, and that between the corresponding transition states TS2 and TS4 is approximately 6.5 kcal/mol. The transition state TS4 has the highest energy level on the surface, which is 39.2 kcal/mol at the uQCISD(T)//uB3LYP/cc-pVDZ level of theory.

The rate constants for the formation of hydroquinoline and hydroisoquinoline were calculated by computer modeling, taking into account the forward and back reactions of INT2 (Figure 2) and INT3 (Figure 3). The back reactions were calculated from the forward reactions and the equilibrium constants between *N*-methyleneindole and the intermediates. The latter were evaluated from the uQCISD(T)//uB3LYP calculations of the

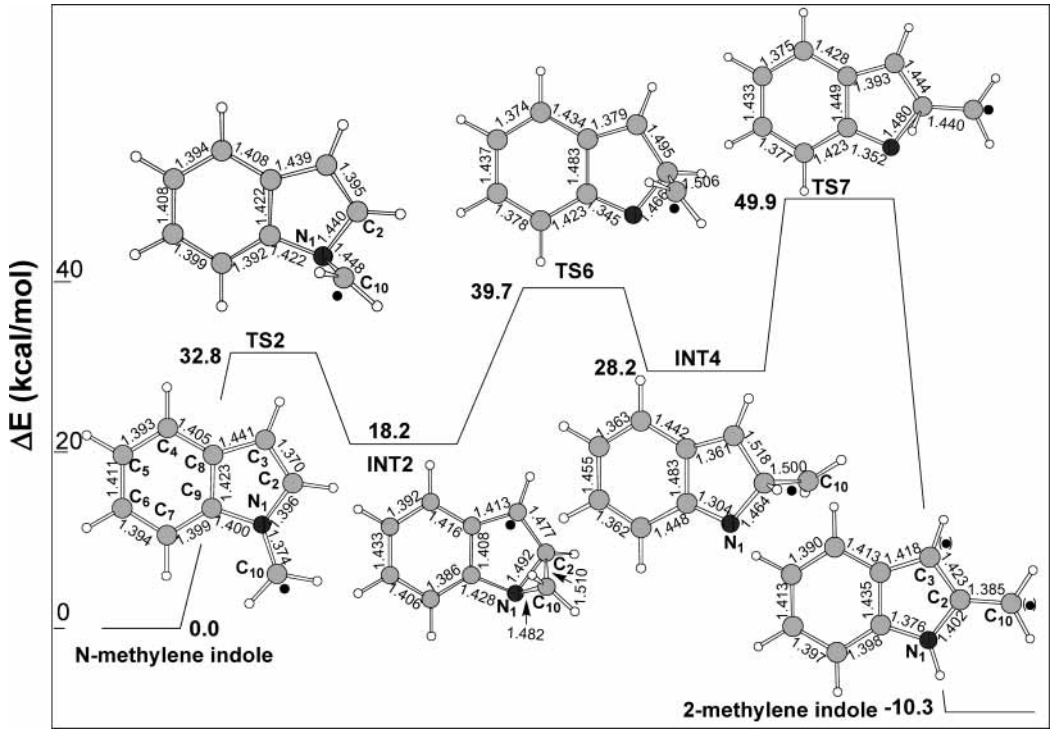

Figure 4. Reaction pathway for *N*-methyleneindole → 2-methyleneindole isomerization. Relative energies (kcal/mol) are calculated at the uQCISD(T)//uB3LYP/cc-pVDZ level of theory. Bond distances are given in angstroms. The symbol (●) denotes partially distributed free electron density.

thermodynamic properties of *N*-methyleneindole and the intermediates. The overall first-order rate constants for each process were calculated from the ratio of [hydroquinoline] to [*N*-methyleneindole] as obtained from the results of the computer modeling at each temperature. The rate constants were then plotted as log *k* vs 1/*T*, and the following Arrhenius parameters were obtained:

$$k_{\text{hydroquinoline}} = 1.62 \times 10^{12} \exp(-31.9 \times 10^3/RT)\ \text{s}^{-1}$$

$$k_{\text{hydroisoquinoline}} = 1.29 \times 10^{12} \exp(-38.2 \times 10^3/RT)\ \text{s}^{-1}$$

where *R* is given in units of cal/(K·mol).

The difference of 6.3 kcal/mol in the barriers on top of a small change in the preexponential factors reflects a ratio of ∼18 at 1200 K between quinoline and isoquinoline. This explains why isoquinoline, which is located between quinoline and *N*-methylindole in the gas chromatogram with a rather poor separation, is not observed in the chromatogram.[1]

2. Isomerizations. *A. Radical Isomerizations. N-Methyleneindole → 2-Methyleneindole.* The potential energy surface of the isomerization is shown in Figure 4. The figure contains selected structural parameters of the species on the surface and the location of the electron density. Some other relevant parameters are listed in Table 1. The isomerization takes place via a shift of the methylene group from N(1) to C(2) and a hydrogen atom from C(2) to N(1).

In the first step, the methylene group forms a bond with C(2), producing a stable intermediate that is identical to INT2 on the ring expansion surface (Figure 2). It has two fused rings, a five-membered and a three-membered ring. However, whereas in the formation of hydroquinoline the bond C(2)−N(1) is broken (Figure 2), in the isomerization process, the bond N(1)−C(10) is broken. The rest of the surface (from INT2 and on) contains two transition states, TS6 and TS7, and one intermediate, INT4 (Figure 4). In TS6, the bond N(1)−C(10) is broken with the formation of an unstable intermediate, INT4, where its benzene ring has completely lost aromaticity. This can be seen in the following scheme:

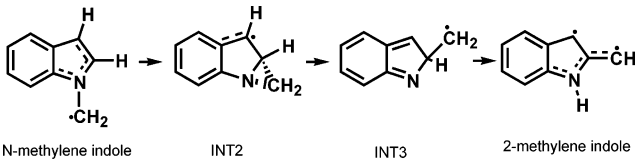

Note that the loss of aromaticity can already be seen in transition state TS6. The energy barrier of this step is ∼22 kcal/mol at the uQCISD(T)//uB3LYP/cc-pVDZ level of theory.

In transition state TS7, there is a 1,2-H-atom shift from C(2) to N(1), forming 2-methyleneindole. The energy level of transition state TS7 is about 22 kcal/mol above that of INT4 and 49.9 kcal/mol above the energy level of *N*-methyleneindole. It is the highest energy level on the surface.

The excess electron density in 2-methyleneindole is almost evenly distributed between C(3) and C(10), whereas in *N*-methyleneindole it is concentrated mainly on C(10). This causes a difference of ∼10 kcal/mol in the stability of two isomers in favor of 2-methyleneindole.

B. Isomerization vs Ring Expansion. Competing Parallel Reactions. It is interesting to point out that the pathways to ring expansion and to *N*-methyleneindole → 2-methyleneindole isomerization compete for the same intermediate, INT2, as can be seen in Figure 5.

Since, however, the barrier for ring expansion from INT2 is much lower than that for isomerization, almost all the *N*-methyleneindole will undergo ring expansion via this mechanism rather than isomerization.

The high yields of 2-methylindole in postshock mixtures of *N*-methylindole suggest that there must be another isomerization mechanism. As will be shown later this interisomerization takes place also from the molecules and not only from the radicals.

C. Molecular Isomerizations. Major components of postshock mixtures of *N*-methylindole are the products of methyl group

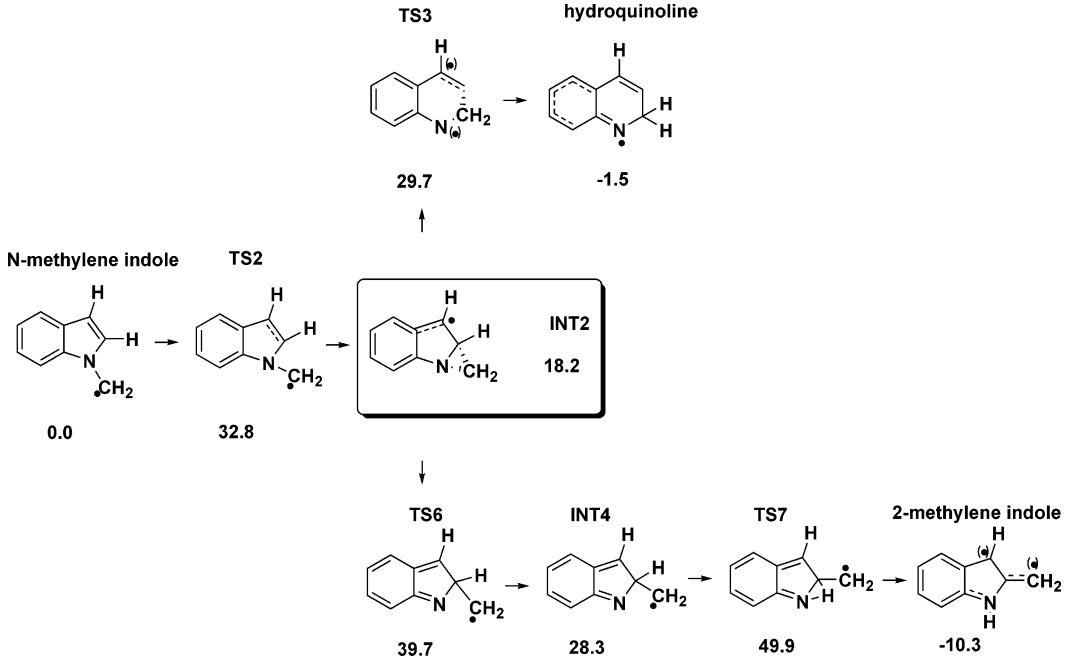

Figure 5. A reaction scheme of both ring expansion and isomerization starting from *N*-methyleneindole. The two processes compete for the same intermediate, INT2.

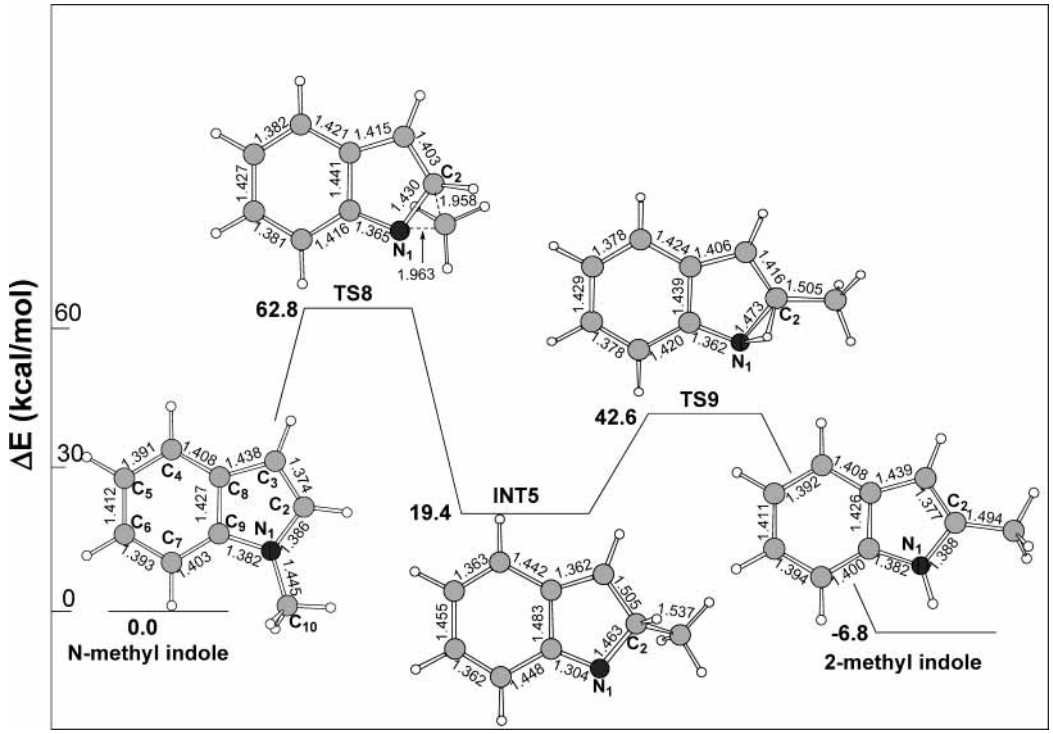

Figure 6. Reaction pathway for *N*-methylindole → 2-methylindole isomerization. Relative energies (kcal/mol) are calculated at the QCISD(T)// B3LYP/cc-pVDZ level of theory. Bond distances are given in angstroms.

shifts. Since the observed experimental isomerization yields could not be accounted for by the rates of the radical isomerizations, we examined the possibility of methyl group shifts directly from the molecule of *N*-methylindole. The observed isomers of *N*-methylindole that were found in postshock mixtures are 2- and/or 3- and 7-methylindole. 2- and 3-methylindole could not be separated in the gas chromatogram.

a. *N*-Methylindole → 2-Methylindole. The potential energy surface of this isomerization is shown in Figure 6, and Table 2 shows the energetics and other parameters on the surface. The surface contains two transition states, TS8 and TS9, and one intermediate, INT5.

The isomerization takes place via 1,2-methyl group migration from N(1) to C(2) and a 1,2-H-atom shift from C(2) to N(1). The first step is the methyl group migration from N(1) to C(2), resulting in the production of an intermediate, INT5. The intermediate has a structure that is characterized by the loss of the aromaticity of the benzene ring, and its energy level is about 19 kcal/mol above that of *N*-methylindole.

The second step is the 1,2-H-atom shift from C(1) to N(1) with the formation of the final product 2-methylindole.

The rate-determining step is the methyl group migration. Its energy barrier is 62.8 kcal/mol, which is practically the energy barrier of the entire process. Although the barrier for the radical

TABLE 2: Total Energies E_{total} (au), Zero-Point Energies, Relative Energies ΔE,[a] Imaginary Frequencies,[b] and Entropies[c] of All the Species on the *N*-Methylindole to 2-Methylindole and 3-Methylindole Isomerization Surfaces, Calculated at the uB3LYP/cc-pVDZ and QCISD(T)/cc-pVDZ//B3LYP/cc-pVDZ Levels of Theory

	uB3LYP					uQCISD(T)	
species	E_{total}	ΔE[a]	ZPE	S[c]	ν[b]	E_{total}	ΔE[a]
			N-Methylindole → 2-Methylindole				
N-methylindole	−403.152772	0.0	98.5	88.0		−401.997574	0.0
TS8	−403.046042	64.9	96.4	85.3	(i-753)	−401.894156	62.8
INT5	−403.111340	25.2	97.7	86.6		−401.965435	19.4
TS9	−403.077012	44.3	95.2	85.9	(i-1417)	−401.924507	42.6
2-methylindole	−403.163428	−6.9	98.3	87.5		−402.007842	−6.8
			N-Methylindole → 3-Methylindole				
N-methylindole	−403.152772	0.0	98.5	88.0		−401.997574	0.0
TS8	−403.046042	64.9	96.4	85.3	(i-753)	−401.894156	62.8
INT5	−403.111340	25.2	97.7	86.6		−401.965435	19.4
TS10	−403.061984	55.1	96.6	85.2	(i-692)	−401.910601	52.7
INT6	−403.140691	7.3	98.1	86.3		not calcd	
TS11	−403.086821	38.4	95.5	85.9	(i-1139)	not calcd	
INT7	−403.115380	22.2	97.2	88.6		not calcd	
TS12	−403.076377	44.6	95.1	87.1	(i-1454)	not calcd	
3-methylindole	−403.160732	−5.1	98.4	87.3		−402.005810	−5.3

[a] Relative energies in kcal/mol. $\Delta E = \Delta E_{total} + \Delta$(ZPE). [b] Imaginary frequencies in cm^{-1}. [c] Entropies at 298 K in cal/(K·mol).

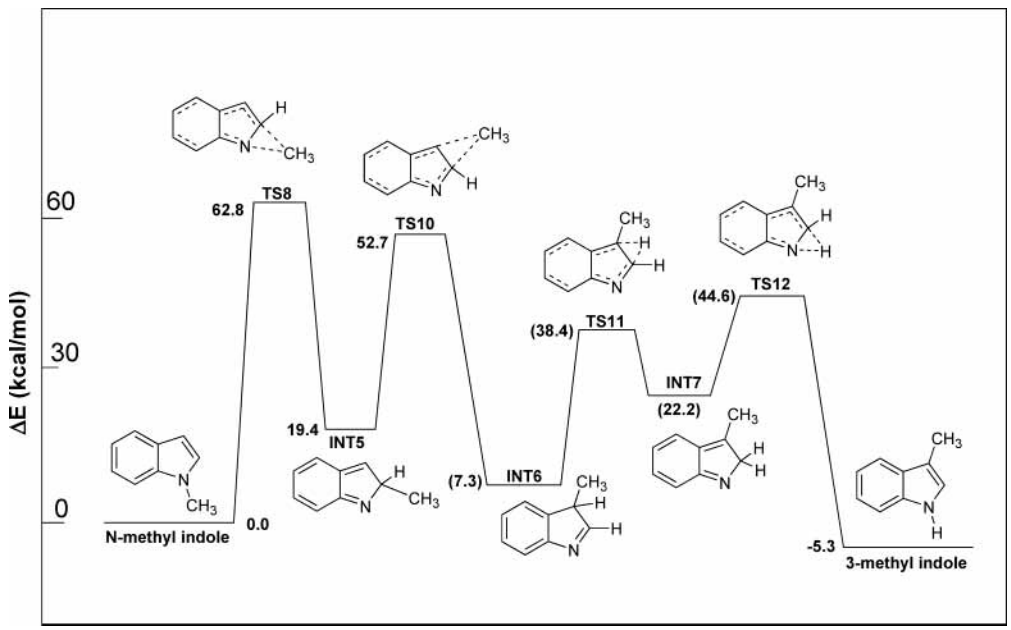

Figure 7. Reaction pathway for *N*-methylindole → 3-methylindole isomerization. Relative energies (kcal/mol) are calculated at the QCISD(T)//B3LYP/cc-pVDZ level of theory; values shown in parentheses are calculated at B3LYP/cc-pVDZ. Bond distances are given in angstroms.

isomerization is lower than the one for the molecular process, the rate of the molecular isomerization is higher because of the unfavored competition between the isomerization process and the ring expansion.

b. *N*-Methylindole → 3-Methylindole. The potential energy surface of this isomerization is shown in Figure 7, and Table 2 shows the energetics and other parameters on the surface. The first step is identical to the one on the *N*-methylindole → 2-methylindole isomerization surface, namely, the production of intermediate INT5 via transition state TS8. To obtain the isomer 3-methylindole, the methyl group should further move from C(2) to C(3), which is the β position relative to nitrogen (INT6). The hydrogen shift from C(3) to N(1) to complete the process is also done in two steps via transition states TS11 and TS12. From a chemical kinetics viewpoint the details of the H-atom transfer are irrelevant since its barriers are considerably below those of the methyl group migrations. (As the QCISD(T) calculations are highly time-consuming they were not done for this part of the surface.) It is interesting to note that the steps on the surface that involve a loss of resonance stabilization have the highest barriers. The highest barrier is the transition from INT5 to INT6 via transition state TS10, which is 52.7 kcal/mol at the QCISD(T)//B3LYP/cc-pVDZ level of theory.

The total scheme for the isomerizations of *N*-methylindole to the 2- and 3- isomers via intermediate INT5 is presented in Figure 8. The figure shows the competition of the two isomers on INT5. Since TS9 is lower in energy by ~10 kcal/mol than TS10, the ratio of the production rates of 2-methylindole to 3-methylindole will be approximately 70 around 1200 K. This could not be verified experimentally, as the two isomers could not be separated properly on the gas chromatograph.

c. *N*-Methylindole → 7-Methylindole. Migration of the methyl group from the nitrogen to one of the carbon atoms of the benzene ring can, in principle, take place as well. We have calculated the potential energy surface of the isomerization to 7-methylindole. The surface is shown in Figure 9. Table 3 shows

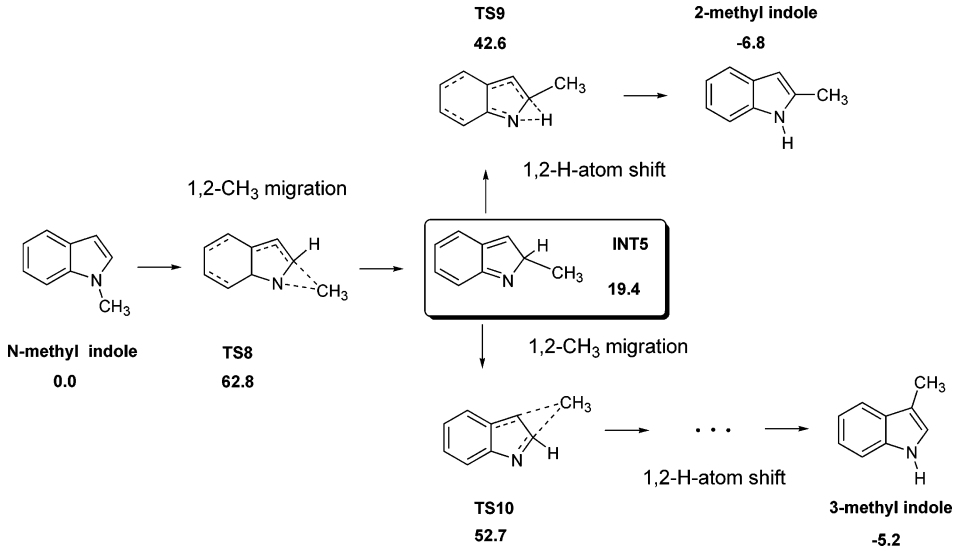

Figure 8. A scheme of *N*-methylindole isomerization to both 2- and 3-methylindole. The two processes proceed via the same intermediate, INT5.

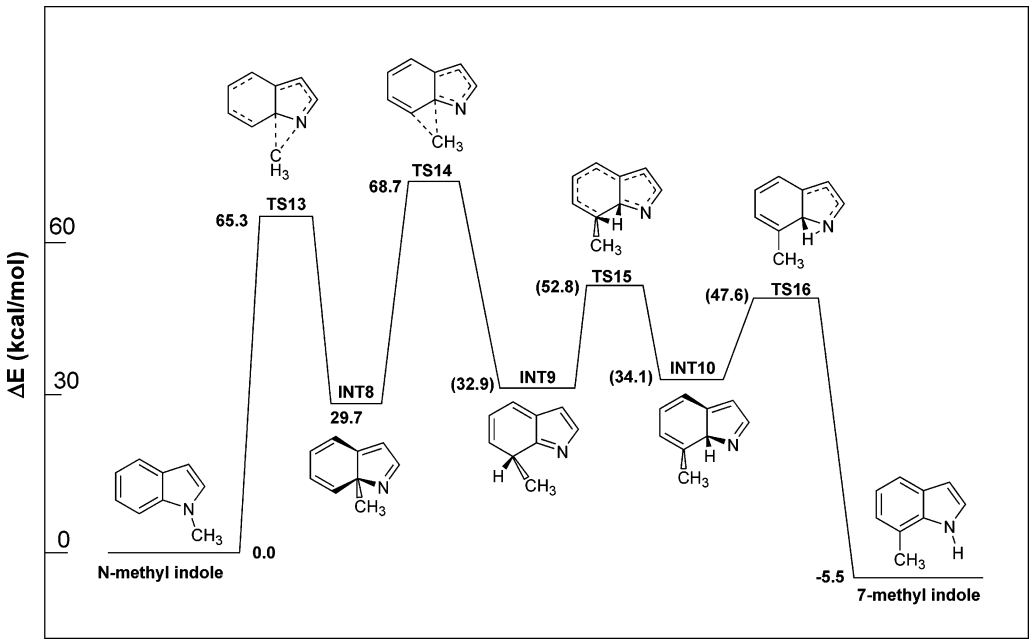

Figure 9. Reaction pathway for *N*-methylindole → 7-methylindole isomerization. Relative energies (kcal/mol) are calculated at the QCISD(T)// B3LYP/cc-pVDZ level of theory; values shown in parentheses are calculated at B3LYP/cc-pVDZ. Bond distances are given in angstroms.

TABLE 3: Total Energies E_{total} (au), Zero-Point Energies, Relative Energies ΔE,[a] Imaginary Frequencies,[b] and Entropies[c] of All the Species on the *N*-Methylindole to 7-Methylindole Isomerization Surface, Calculated at the uB3LYP/cc-pVDZ and QCISD(T)/cc-pVDZ//B3LYP/cc-pVDZ Levels of Theory

	uB3LYP					uQCISD(T)	
species	E_{total}	ΔE^a	ZPE	S^c	ν^b	E_{total}	ΔE^a
N-methylindole	−403.152772	0.0	98.5	88.0		−401.997574	0.0
TS13	−403.039569	68.7	96.1	86.3	(i-679)	−401.889698	65.3
INT8	−403.086945	40.3	97.4	85.5		−401.948657	29.7
TS14	−403.035501	71.2	96.0	86.5	(i-677)	−401.884198	68.7
INT9	−403.098850	32.9	97.5	87.6		not calcd	
TS15	−403.063003	52.8	94.9	86.1	(i-1087)	not calcd	
INT10	−403.096330	34.1	97.2	86.9		not calcd	
TS16	−403.071613	47.6	95.2	86.1	(i-1346)	not calcd	
7-methylindole	−403.160396	−4.9	98.3	87.1		−402.006351	−5.5

[a] Relative energies in kcal/mol. $\Delta E = \Delta E_{total} + \Delta(ZPE)$. [b] Imaginary frequencies in cm^{-1}. [c] Entropies at 298 K in cal/(K·mol).

the energetics and other parameters on the surface. It should be mentioned that since the H-atom shifts have considerably lower barriers than the methyl group migrations, we have not performed configuration interaction calculations (QCISD(T)) for the H-atom shifts as from a kinetics viewpoint they are irrelevant. An important feature in the surface is the destruction

of the aromatic stabilization of both of the benzene and the pyrrole rings. The highest barrier on the surface is considerably higher than the corresponding barriers of the isomerization processes where the methyl group stays in the pyrrole ring. The highest barrier on the surface is 68.7 kcal/mol, and it corresponds to methyl group migration from C(9) to C(7). It is expected therefore that the yields of the 7-isomer will be much lower than those of the 2- and 3-isomers. This observation is supported by the experimental results.[1]

d. Isomerization Rate Constants. The rate constant for isomerization of *N*-methylindole to 2-methylindole was calculated using computer modeling, taking into account all the elementary steps on the potential energy surface as is shown in Figure 6. It is interesting to note that the results of these calculations were practically identical to a calculation where *N*-methylindole goes directly to 2-methylindole in one step via transition state TS8; namely, the first step on the potential energy surface (Figure 6) is rate determining. The rate constant obtained is

$$k_{1\rightarrow\text{2-methylindole}} = 1.15 \times 10^{13} \exp(-64.2 \times 10^3/RT)\ \text{s}^{-1}$$

where R is given in units of cal/(K·mol). Another interesting observation is that 2-methylindole and INT5 reach a state of equilibrium as of the early stages of the isomerization.

As has been mentioned before, the isomerization of *N*-methylindole to 3-methylindole goes via intermediate INT5, which is also the first step in the isomerization of *N*-methylindole to 2-methylindole. From this stage on there are two competing parallel reactions to form 2- and 3-methylindole. However, since the barrier to produce 2-methylindole involves only H-atom migration and the one to form 3-methylindole involves both methyl group and H-atom migrations, the barrier of the latter is higher by 10 kcal/mol, which would normally mean that most of INT5 will go to 2-methylindole. However, since 2-methylindole and INT5 reach a state of equilibrium, the competition ceases to exist and the formation rate of 3-methylindole is determined solely by the production rate of INT5. It is interesting to note that the state of equilibrium between 2-methylindole and INT5 is not perturbed by the existence of the channel that produces 3-methylindole as the latter is much slower than the rate of attainment of the equilibrium. The rate constant obtained for the two isomerizations is given by

$$k_{\text{2- and 3-methylindole}} = 6.29 \times 10^{12} \exp(-63.0 \times 10^3/RT)\ \text{s}^{-1}$$

where R is expressed in units of cal/(K·mol).

The rate constant of the isomerization from *N*-methylindole to 7-methylindole was calculated by computer modeling, taking into account the first two steps on its potential energy surface (Figure 9). The value obtained is

$$k_{\text{7-methylindole}} = 7.30 \times 10^{12} \exp(-70.2 \times 10^3/RT)\ \text{s}^{-1}$$

where R is given again in units of cal/(K·mol).

The comparison between the calculated and the experimental results[1] is shown in Figure 10. As can be seen the calculated barriers are somewhat higher than the experimental ones. Assuming the same preexponential factors for the experimental and calculated values, the calculated energy barrier for the production of 2-methylindole is higher by ~4 kcal/mol than the experimental one and by ~2 kcal/mol for the production of 7-methylindole.

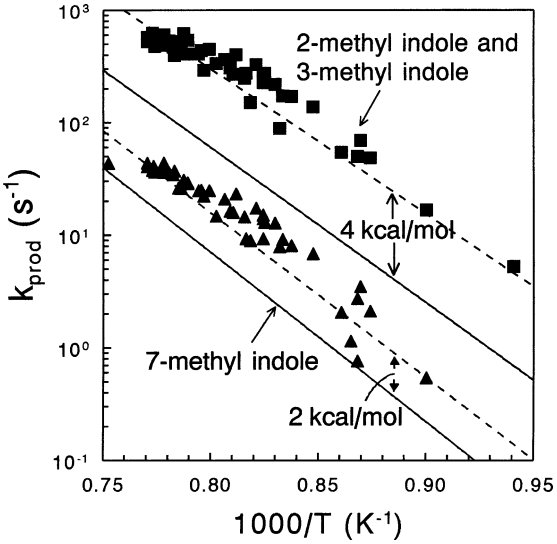

Figure 10. Arrhenius plots of the calculated rate constants of *N*-methylindole → 2- and 3-methylindole and *N*-methylindole → 7-methylindole isomerizations. The experimental data are presented as squares for 2- and 3-methylindole and as triangles for the production of 7-methylindole. The solid lines are the results of the calculations, and the dotted lines represent adjustments by 4 kcal/mol for the production of 2- and 3-methylindole and 2 kcal/mol for the production of 7-methylindole to fit the experimental results.

IV. Common Features in Ring Expansion and Isomerization of Five-Membered Rings

The quantum chemical calculations of ring expansion and isomerization of *N*-methylindole presented in this paper complement a series of similar calculations of ring expansion and isomerization in other five-membered rings, with and without nitrogen as a heteroatom: methylpyrrole, methylcyclopentadiene, and methylindene. The following features are common to all of these compounds.

The lowest energy pathways for ring expansion are in the isomers where the methylene group is connected to an sp^3 carbon or nitrogen. The other isomers undergo ring expansion via isomerization to N- or sp^3-substituted radicals, rather than via direct reaction.

The processes in the five-membered rings containing nitrogen have higher barriers than those in the five-membered rings without nitrogen. This is caused by a considerable loss of aromaticity of the pyrrole ring in the transition states and intermediates.

The fused benzene ring increases the barriers only when there is a loss of aromaticity in the intermediates.

The energy barrier for the production of isoquinoline from *N*-methyleneindole is higher than that for quinoline, owing to the formation of an intermediate with three rings fused together.

Ring expansion from the molecules has barriers that are much higher than those from their respective radicals. This results from the fact that the process in the molecules involves in the first stage two simultaneous processes: N−C bond cleavage and H-atom ejection.

Acknowledgment. This research was supported by The Israel Science Foundation (ISF Grant No. 34/01).

References and Notes

(1) Lifshitz, A.; Tamburu, C.; Suslensky, A. Decomposition of methyl indole, unpublished results (in preparation for submission to *J. Phys. Chem. A*).
(2) Dubnikova, F.; Lifshitz, A. *J. Phys. Chem. A* **2000**, *104*, 530.
(3) Dubnikova, F.; Lifshitz, A. *J. Phys. Chem. A* **2002**, *106*, 8173.

(4) Lifshitz, A.; Tamburu, C.; Suslensky, A.; Dubnikova, F. *J. Phys. Chem. A* **2004**, *108*, 3436.
(5) Dubnikova, F.; Lifshitz, A. *Isr. J. Chem.* **2003**, *43*, 325.
(6) Becke, A. D. *J. Chem. Phys.* **1993**, *98*, 5648.
(7) Lee, C.; Yang, W.; Parr, R. G. *Phys. Rev.* **1988**, *B37*, 785.
(8) Dunning, T. H. Jr. *J. Chem. Phys.* **1989**, *90*, 1007.
(9) Schlegel, H. B. *J. Comput. Chem.* **1982**, *3*, 214.
(10) Peng, C.; Schlegel, H. B. *Isr. J. Chem.* **1993**, *33*, 449.
(11) Pople, J. A.; Head-Gordon, M.; Raghavachari, K. J. *J. Chem. Phys.* **1987**, *87*, 5968.
(12) Frisch, M. J.; Trucks, G. W.; Schlegel, H. B.; Scuseria, G. E.; Robb, M. A.; Cheeseman, J. R.; Zakrzewski, V. G.; Montgomery, J. A., Jr.; Stratmann, R. E.; Burant, J. C.; Dapprich, S.; Millam, J. M.; Daniels, A. D.; Kudin, K. N.; Strain, M. C.; Farkas, O.; Tomasi, J.; Barone, V.; Cossi, M.; Cammi, R.; Mennucci, B.; Pomelli, C.; Adamo, C.; Clifford, S.; Ochterski, J.; Petersson, G. A.; Ayala, P. Y.; Cui, Q.; Morokuma, K.; Malick, D. K.; Rabuck, A. D.; Raghavachari, K.; Foresman, J. B.; Cioslowski, J.; Ortiz, J. V.; Stefanov, B. B.; Liu, G.; Liashenko, A.; Piskorz, P.; Komaromi, I.; Gomperts, R.; Martin, R. L.; Fox, D. J.; Keith, T.; Al-Laham, M. A.; Peng, C. Y.; Nanayakkara, A.; Gonzalez, C.; Challacombe, M.; Gill, P. M. W.; Johnson, B. G.; Chen, W.; Wong, M. W.; Andres, J. L.; Head-Gordon, M.; Replogle, E. S.; Pople, J. A. *Gaussian 98*, revision A.7; Gaussian, Inc.: Pittsburgh, PA, 1998.
(13) Eyring, H. *J. Chem. Phys.* **1935**, *3*, 107.
(14) Evans, M. G.; Polanyi, M. *Trans. Faraday Soc.* **1935**, *31*, 875.